LWT - Food Science and Technology 239 (2026) 118896

Contents lists available at ScienceDirect

LWT

journal homepage: www.elsevier.com/locate/lwt

Preparation, characterization, and oxidative stability of black soybean oil body-based oleogels

Jie Sun [a], Cuicui Fan [a], Guoyou Yin [a,*], Zhuofan Yang [a], Yulin Liu [a], Jing Lu [b]

[a] College of Life Science and Engineering, Henan University of Urban Construction, Pingdingshan, 467036, China
[b] Department of Molecular Sciences, Swedish University of Agricultural Sciences (SLU), P.O. BOX 7015, 75007, Uppsala, Sweden

ARTICLE INFO

Keywords:
black soybean oil body (BSOB)
Anionic polysaccharide
Oleogels properties
Oxidation stability

ABSTRACT

Oil bodies (OBs) are natural emulsions existing in the form of proteins wrapping liquid oil. Due to their environmentally friendly extraction process, rich nutrition, and natural emulsification characteristics, OB exhibits great potential for application in the food industry. In this study, we combined black soybean oil body (BSOB) emulsion separately with four anionic polysaccharides including carrageenan (C), pectin (P), sodium alginate (S), and xanthan (X) through electrostatic deposition. We then prepared BSOB-based oleogels using the emulsion template method. Additionally, we evaluated the microstructure and physical properties of the oleogels such as oil holding capacity, texture, rheological properties, and oxidative stability using confocal laser scanning microscope (CLSM), a rheometer, texture analyzer, differential scanning calorimeter, and other instruments. The results showed that the electrostatic interaction between anionic polysaccharides and BSOB emulsion reduced BSOB aggregation and increased BSOB stability, thus reducing the leakage of oil droplets in BSOB from the three-dimensional (3D) structure during the freeze-drying process. After adding anionic polysaccharides, the gel strength of the oleogels improved, and the oil holding capacity and oxidation stability also significantly increased ($P < 0.05$). Furthermore, the thermal stability of the oleogels formed by BSOB and carrageenan was higher than those formed with other anionic polysaccharides, potentially due to its high ζ-potential value of electrostatic interaction (−33.87 mV). Overall, this study proposes a novel strategy for preparing black bean oil bodies into stable new oleogels, providing a new perspective for replacing artificial solid fats with natural oil bodies.

1. Introduction

Fats contain large amount of saturated and trans fatty acids (Martins et al., 2018; Zembyla et al., 2020), and excessive fat intake can lead to multiple diseases such as coronary heart disease, atherosclerosis, type II diabetes, and obesity. Particularly, excessive intake of trans fats is considered a major cause of the high morbidity and mortality associated with cardiovascular disease (Restrepo & Rieger, 2015). Mozaffarian et al. (2006) reported that consumption of processed foods rich in saturated and artificial trans fats could increase the prevalence of coronary heart disease from 23 % to 29 %. By 2023, trans fatty acids have been required to be eliminated from the global food supply, with limits also placed on saturated fatty acid contents (Astrup et al., 2020). The World Health Organization recommends replacing the solid fats containing saturated and trans fatty acids in processed foods with healthier vegetable oils containing unsaturated fatty acids. However, vegetable oils can damage the textural and structural properties of food, usually resulting in greasy and less crispy food products, as well as shortened shelf life due to oil oxidation (Demirkesen & Mert, 2020; Patel et al., 2020). Although trans fatty acids in solid fats can effectively promote and stabilize the formation of a three-dimensional network crystal structure during fat crystallization, it remains challenging to replace solid fats with liquid oils while maintaining food quality. Thus, achieving desirable food qualities by replacing solid fats with liquid oils is challenging. In recent years, oleogelation has emerged as an effective strategy for replacing trans and saturated fats by developing soft solid structures from edible oils without altering their chemical properties (Bascuas et al., 2021).

Although oleogels can replace trans and saturated fatty acids in food, maintaining the sensory properties, oxidative stability, and physicochemical properties of food products remains a challenge (Singh, Auzanneau, & Rogers, 2017). Recently, the use of polysaccharides as gelling agents has attracted widespread attention because they compensate for the shortcomings of other gelling agents. For example,

* Corresponding author.
E-mail address: 30110605@huuc.edu.cn (G. Yin).

https://doi.org/10.1016/j.lwt.2025.118896
Received 20 August 2025; Received in revised form 6 December 2025; Accepted 9 December 2025
Available online 10 December 2025

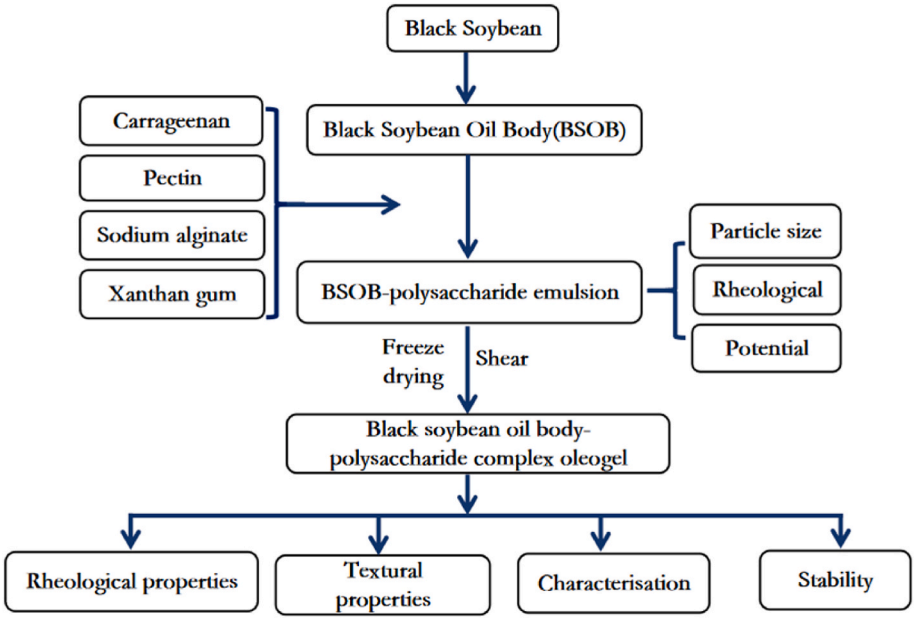

Fig. 1. Experimental design.

polysaccharides require lower concentrations and temperatures to form oleogels (Bascuas et al., 2021), and being derived from renewable sources, they are cost-effective and popular with consumers (Meng et al., 2018a). Despite their hydrophilicity, the high molecular weight of polysaccharides allows them to gel at low concentrations, thus meeting most of the criteria for effective gelling agents (Davidovich-Pinhas M., 2019). The method for preparing oleogels using polysaccharides involves mixing polysaccharides, proteins, and liquid oil to form emulsion, which is then freeze-dried to remove water, and finally sheared to form oleogels.

Stable artificial emulsions are prepared by high-pressure homogenization or high-shear treatment. For sustainability and economic reasons, natural emulsions have become a potential alternative to traditional artificial emulsions. Oil bodies (OBs) are natural emulsions existing in the form of proteins wrapping liquid oils, and using OBs can reduce the steps required to form emulsions. OBs are primarily derived from a variety of plants (Huang, 2018), microorganisms such as bacteria, yeasts, and microalgae (Wältermann and Steinbüchel, 2005), and mammals (Barbosa & Siniossoglou, 2017). Research interested in plant OBs has increased as they offer multiple advantages such as easy extraction, high yield recovery, and safety in food use, meeting consumers' demand for all-natural products. Although OBs are found in various parts of plants, such as seeds, leaves, and roots (Shimada & Hara-Nishimura, 2015), they are mainly located in the cell tissues of seeds and nuts (Liu et al., 2020; Romero-Guzmán et al., 2020).

Black beans contain many ingredients beneficial to human health, including lipids, vitamins, proteins, and trace elements (Ferreira et al., 2018). High in nutrition and low in calories, black beans are particularly beneficial for weight loss. High-levels of unsaturated fats in black beans can help reduce the risk of cardiovascular disease. Additionally, isoflavones, trace elements, and dietary fiber in black beans offer medical benefits, such as delaying aging, reducing blood viscosity, preventing constipation, and improving resistance to obesity and hypolipidemia (Lima et al., 2014). However, there have been few reports on the research and development of black soybean oil bodies (BSOB).

Exploring the gelation mechanism, physicochemical properties, and functions of BSOB-based oleogels is of great significance to promote their application in health foods. Therefore, in this study, four common anionic polysaccharides including carrageenan (C), pectin (P), xanthan (X), and sodium alginate (S)were used to prepare BSOB-based oleogels using electrostatic deposition technology. The effects of different anionic polysaccharides on BSOB-based oleogels were investigated by comparing their average particle size, ζ-potential, oil holding property, thermal stability, rheological property, and texture property (Fig. 1). The application potential of BSOB-based oleogels as a solid fat substitute was evaluated based on their oxidative stability. Overall, this study provides a theoretical basis for the preparation and application of new oil body oleogels.

2. Materials and methods

2.1. Materials and chemicals

Black beans were purchased from a supermarket in Jiamusi, China. Carrageenan, pectin, sodium alginate and xanthan gum were provided by Henan Qihuali Biotechnology Co., Ltd. Zhengzhou, China. Nile Blue and Nile Red were purchased from Sigma Aldrich Trading Co., Ltd., Shanghai and Shanghai Aladdin Biochemical Technology Co., Ltd., respectively. All other reagents were of analytical grade.

2.2. Extraction of BSOB

BSOB was prepared according to a previously reported method (Chen & Ono, 2010). Specifically, black soybeans were soaked in distilled water for 12–14 h, crushed, and filtered to obtain filtrate. The pH of the filtrate was adjusted to 11 using 1 M NaOH and was then centrifuged at 10,000×*g* for 30 min at 4 °C, and the upper OB-rich layer was collected and re-mixed with a 20 % (w/w) sucrose solution and centrifuged at 10,000×*g* for 30 min at 4 °C after adjusting the pH to 11.0. After centrifugation, the upper layer was collected to obtain BSOB.

2.3. Preparation of BSOB-based oleogels

The BSOB-based oleogels was prepared with slight modifications to a previously reported method (Mert and Vilgis, 2021). Specifically, 75 g of BSOB was added to 100 mL of ultrapure water and stirred at 600 rpm for 30 min. The pH was adjusted to 4.0 using 1 M HCl. The BSOB emulsion was then mixed with various concentrations of polysaccharide solution (0.5 wt%, 1.0 wt%, 1.5 wt%, and 2.0 wt%), and treated with a high-speed disperser (Aika Instrument Equipment Co., LTD, Guangzhou,

China) for 4 min. The pH was adjusted to 7.0 using 1 M NaOH. After 48 h of vacuum freeze-drying, the freeze-dried samples were sheared with a tissue crusher for 3 min to form oleogels. The resultant oleogels samples were categorized as follows: (1) BSOB (without polysaccharide), (2) BSOB-C0.5, BSOB-C1.0, BSOB-C1.5, and BSOB-C2.0 (containing 0.5 %, 1.0 %, 1.5 %, and 2.0 % carrageenan, respectively), (3) BSOB-P0.5, BSOB-P1.0, BSOB-P1.5, and BSOB-P2.0 (containing 0.5 %, 1.0 %, 1.5 %, and 2.0 % pectin, respectively), (4) BSOB-S0.5, BSOB-S1.0, BSOB-P1.5, and BSOB-P2.0 (containing 0.5 %, 1.0 %, 1.5 %, and 2.0 % sodium alginate, respectively), (5) BSOB-X0.5, BSOB-X1.0, BSOB-X1.5, and BSOB-X2.0 (containing 0.5 %, 1.0 %, 1.5 %, and 2.0 % xanthan, respectively). The oleogels samples were stored at 4 °C for subsequent use.

2.4. Measurement of potential and particle size

The potential and particle size of the BSOB-polysaccharide emulsions were measured referring to a previously reported method (Zambrano & Vilgis, 2023). Briefly, the mixed emulsion was diluted with 10 mM PBS (pH 7) to reach a BSOB concentration of 0.05 wt%. Measurements were conducted at 25 °C, adjusting the refraction rate of the samples and the dispersed phase to 1.59 and 1.33, respectively.

2.5. Rheological properties

The viscosity of the BSOB-polysaccharide emulsion was characterized using a rheometer (Thermo Fisher Technologies, German). A PP35Ti cone-plate was used with a shear rate range from 0.1 to 100.0 s^{-1} and a gap of 1 mm at a constant temperature of 25 °C. The oleogels samples were measured using a method reported by Abdollahi et al. (2020). Specifically, a C35 2°Ti L cone plate was used with a gap of 2 mm, and the temperature was adjusted to 25 °C using a Peltier system circulating water bath and kept constant. A thin layer of low-viscosity silicone oil was placed on the surface of the oleogels between the two plates to prevent water loss during the measurement. A frequency sweep (0.1–100.0 Hz,25 °C) was performed at a strain amplitude of 0.5 % with sequential shear rates of 0.1 s^{-1}, 10 s^{-1}, and 0.1 s^{-1} for 1 min each to evaluate the thixotropy of the oleogels samples.

2.6. Textural properties

After compression, the texture properties of the samples were analyzed using a method reported by Luo et al. (Luo et al., 2019) with slight modifications. The texture of the freeze-dried product was determined using a P/36R probe with a pre-test speed of 5.0 mm/s, a test speed of 1.0 mm/s, a post-test speed of 5.0 mm/s, a trigger force of 5.0 g, and a compression deformation of 75 %. Likewise, the texture of the oleogels (after shearing of the freeze-dried samples) was tested using a P/0.5 probe with a pre-test speed, a test speed, and a post-test speed of 1 mm/s, respectively, and a test deformation and trigger force of 60 % and 5.0 g, respectively.

2.7. Confocal laser scanning microscopy observation

The microscopic morphology of the oleogels was observed using a confocal laser scanning microscope (LSM710 CLSM, Germany Leica Instrument Co., Ltd, Germany) at 40× magnification. Before imaging, the oleogels were mixed with dyes Nile blue and Nile red to stain proteins and lipids, respectively. The excitation wavelengths of Nile blue and Nile red was set as 633 nm and 488 nm, respectively.

2.8. Thermal stability determination

The thermal properties of oleogels were evaluated using a Q2000 differential scanning calorimetry (American TA Instruments Ltd, USA). 10 mg of oleogels samples were placed into an alumina crucible. The scanning temperature range was set as 30 °C–160 °C, and both the heating rate and cooling rate were set as 10 °C/min. The detection process was protected by N_2, with a gas flow rate of 50 mL/min.

2.9. Determination of oil loss

The oil loss from the oleogels was calculated by the centrifugation method reported by Farooq et al. (2022). A 2 g oleogels sample was centrifuged in a centrifugate bottle at 20 °C and 10,000 rpm for 15 min to remove excess oil. Then, the oil loss was calculated by measuring the weight of the remaining oleogels according to the following formula:

$$\text{Oil loss rate } (\%) = \frac{(w_1 - w) - (w_2 - w)}{w_1 - w} \times 100$$

Where W is the weight of the centrifuge bottle; W_1 is the weight of the sample with the centrifuge bottle; and W_2 is the weight of the oleogels with the centrifuge bottle.

2.10. Oxidative stability determination

The oleogels samples were stored in a 60 °C thermostat for 7 days, and an accelerated oxidation experiment was performed. The hydroperoxide and thiobarbituric acid reactant contents in the samples were measured at the same time point every day (Zhu et al., 2022).

2.10.1. Determination of peroxide value (POV) of primary oxidation products

The peroxide value (POV) of primary oxidation products was determined using the method reported by Aberkane et al. (2014). Briefly, 0.1 g of oleogels was dissolved in 1 mL of distilled water and mixed thoroughly to prepare the emulsion. Then, 0.3 mL of resultant emulsion was added into 1.5 mL mixture of isooctane and isopropanol (at a ratio of 3:1, v/v), shaken thoroughly (for 3 times, 10 s per time), and centrifuged at 5000 g for 2 min. Subsequently, 0.2 mL of the supernatant was taken and added into 2.8 mL of methanol-butanol mixture (2:1, v/v), and then the mixed solution was separately added with 20 μL of 3.94 mol/L ammonium thiocyanate and 20 μL of Fe^{2+} solution (containing 0.132 mol/L $BaCl_2$ and 0.144 mol/L $FeSO_4$ at a ratio of 1:1), mixed thoroughly, and reacted in the dark for 20 min to measure the absorbance at 510 nm. The different concentrations of standard solutions (50, 100, 200, 300, 400, 500 μmol/L) were prepared using 30 % hydrogen peroxide solution for standard curve plotting.

2.10.2. Determination of thiobarbituric acid reaction substance (TBARS)

The thiobarbituric acid reaction substance (TBARS) as secondary oxidation products was determined, referring to the method reported by Ding et al. Briefly, 0.1 g of oleogels was taken and added into 4 mL of TBARS test solution (containing 0.375 % thiobarbituric acid, 15 % trichloroacetic acid, and 0.25 mol/L HCl). The mixture solution was first heated in boiling water for 20 min, then cooled in ice water for 10 min, and centrifuged at 8000 g for 15 min. Afterwards, the supernatant was taken to measure the absorbance at 532 nm. The concentration of TBARS in the samples was calculated according to the 1,1,3,3-tetraethoxypropane standard curve.

2.11. Statistical analysis

All the experiments were conducted with 5 technical replicates unless stated otherwise. The Origin 2022 (Origin lab Software Corp, Northampton, MA, USA) was used for plotting, and the Duncan's test was performed using IBM SPSS 25 (IBM Inc., Armonk, NY, USA) software to determine the significant difference ($P < 0.05$).

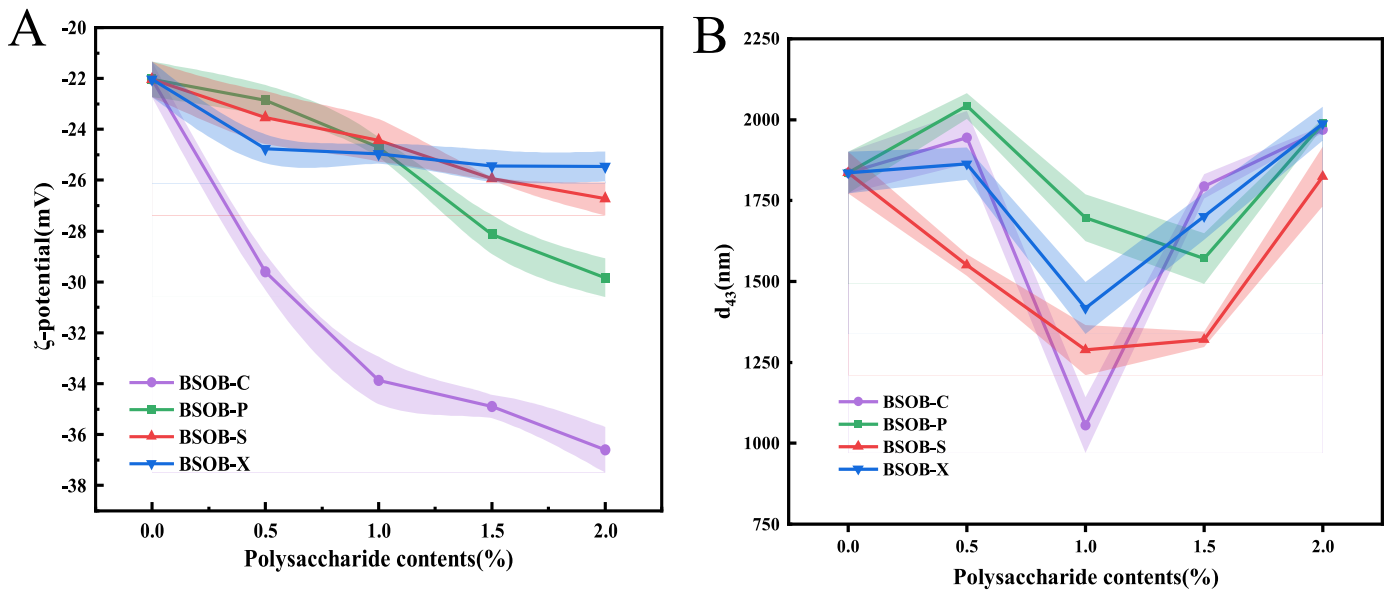

Fig. 2. Effects of different concentrations of k-carrageenan, pectin, sodium alginate and xanthan gum onζ-potential and average particle size of BSOB-polysaccharide emulsions.

3. Results and discussion

3.1. The analysis of ζ-potential and particle size of different BSOB-polysaccharide emulsion

BSOB coated with different concentrations of C, P, S, and X (0 %, 0.5 %, 1.0 %, 1.5 %, 2.0 %) were prepared, and their ζ-potential values and particle sizes were measured. With increasing concentration of the four anionic polysaccharides, the ζ-potential values of coated BSOB continued to decrease, particularly for BSOB-C(Fig. 2A). The average particle sizes of BSOB-C, BSOB-P, and BSOB-X fluctuated, with initially increasing, then decreasing to a minimum value, before increasing again (Fig. 2B). Specially, when the polysaccharide concentration increased from 0.0 wt % to 0.5 wt %, the average particle size of the coated BSOB emulsion also increased. This increase could be attributed to the reduced ζ-potential and weakened electrostatic repulsion between BSOB at lower polysaccharide concentrations. Additionally, individual polysaccharide molecules may have adsorbed onto the surface of multiple OBs, leading to cross-linking of the compounds (Wu et al., 2022). The particle sizes of these three coated BSOB emulsions decreased as the charged polysaccharides were continuously electrostatically adsorbed onto the BSOB surface, enhancing electrostatic repulsion and steric hindrance, thereby resisting aggregation and improving stability (Yang et al., 2023). Notably, after the average particle size reached its minimum, it began to increase again due to increased interaction resulting in flocculation and strengthened dispersed droplet network structure at high polysaccharide concentration (Zhu et al., 2024). Particularly, at a 1.0 % polysaccharide concentration, the average particle size of BSOB-C reached the minimum value (1055 nm), and the absolute ζ-potential was 33.86 mV. the denser charged helical structure of BSOB-C likely

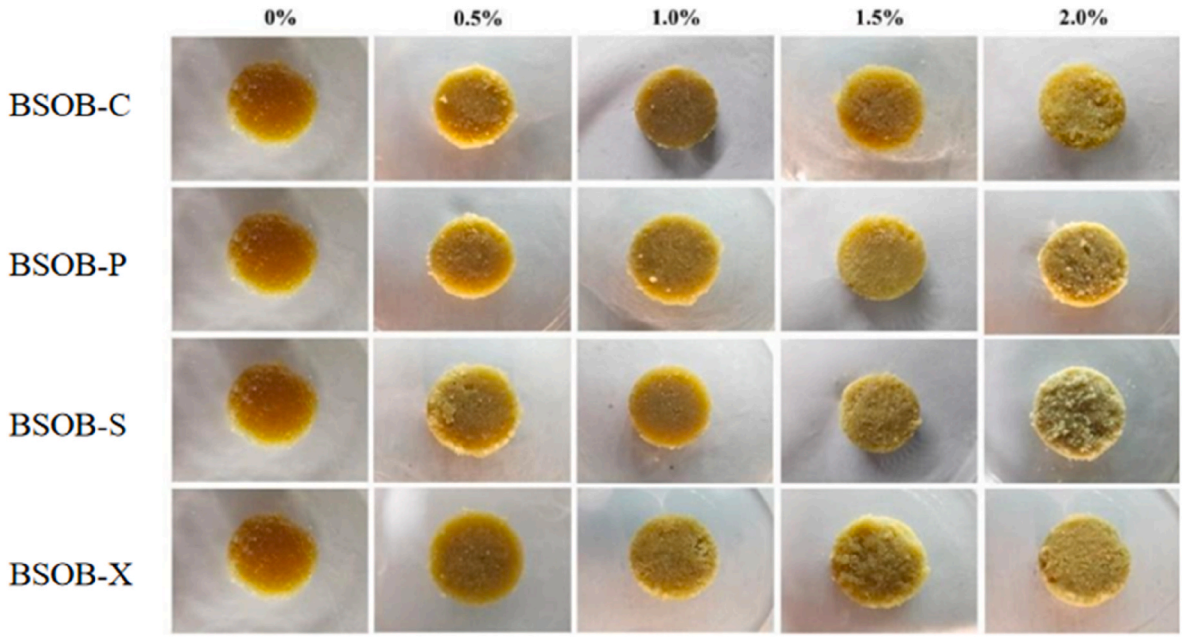

Fig. 3. The visual images of oleogels obtained by using different concentrations (0 %, 0.5 %, 1.0 %, 1.5 % and 2.0 %) of anionic polysaccharides.

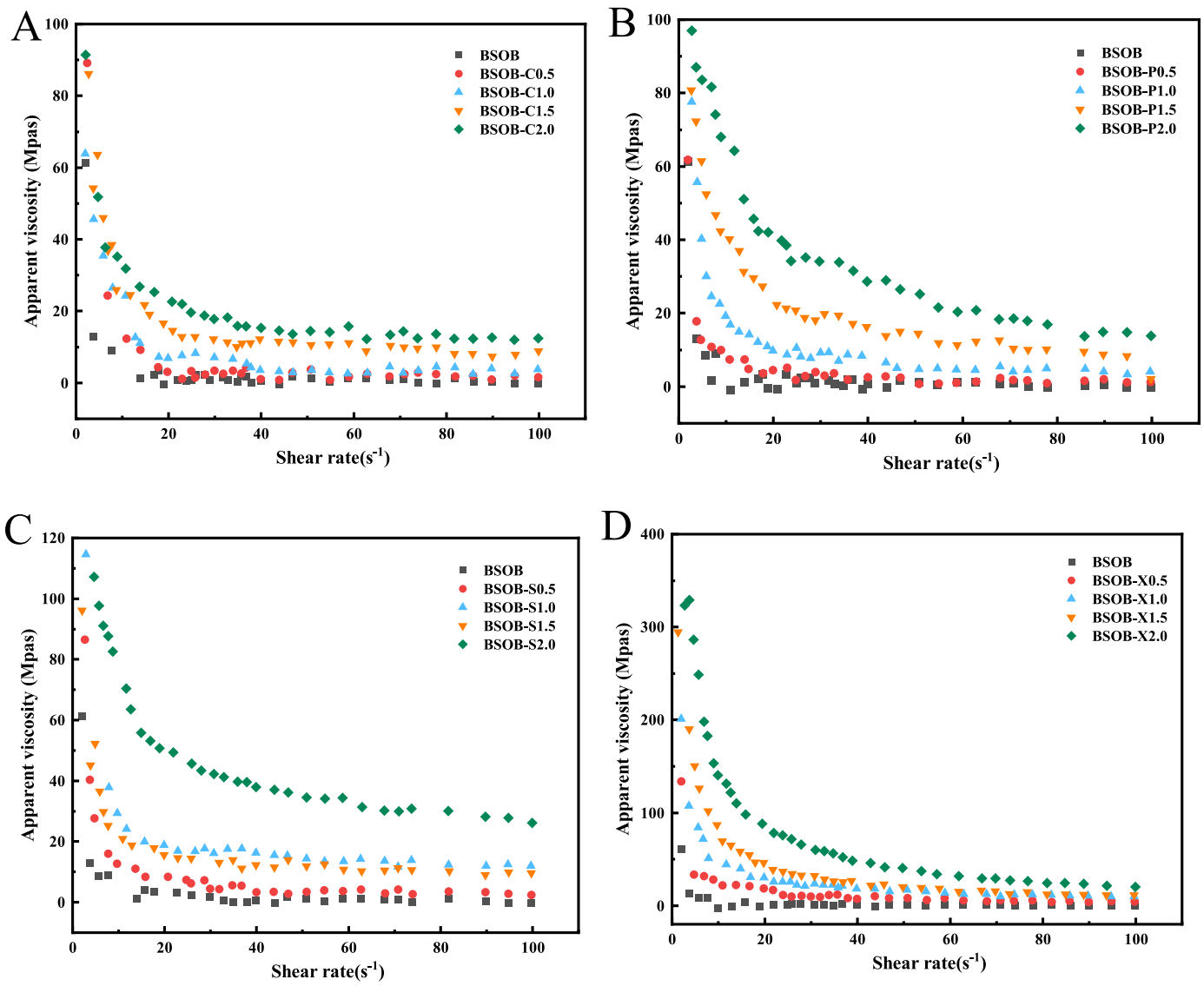

Fig. 4. Variation curve of apparent viscosity of BSOB-polysaccharide emulsion with shear rate.

formed a highly charged interface membrane, effectively reducing flocculation depletion (Wu et al., 2011). Furthermore, a ζ-potential greater than 30 mV (Fig. 2A) indicates superior stability as the dispersed oil bodies repelled each other to hinder aggregation. These findings are consistent with previous reports (Meng et al., 2018a; Zhu et al., 2024). Compared to the other polysaccharides, the average particle size of the BSOB-S emulsion significantly decreased when the concentration increased from 0.0 wt % to 1.0 wt %. Sodium alginate, due to its flexible polymer chain structure, forms a negatively charged interfacial protective layer on the surface of oil droplets. Sufficient electrostatic repulsion is generated among oil-body particles, thereby maintaining emulsion stability and preventing aggregation (Zhang et al., 2019). As the concentration continued to increase, the average particle size of BSOB-S gradually increased, but its stability decreased, possibly due to flocculation depletion by high-level unabsorbed S in the continuous phase (Su et al., 2018).

3.2. *Visual appearance analysis of oleogels*

Fig. 3 shows the appearance of oleogels prepared from various concentrations of anionic polysaccharides combined with BSOB. The dried sample mixtures were sheared into pieces to form oleogels, which appeared as granular aggregates with liquid oil trapped within. The oleogels were not easy to flow, exhibiting a semi-solid appearance. After the freeze-dried sample mixtures were sheared, obvious oil precipitation was observed; when the concentration of anionic polysaccharides was <1.0 %, the texture of the oleogels with different types of anionic polysaccharides was softer, but there was still a small amount of oil on the oleogels surface; when the anionic polysaccharide concentration was ≥1.0 %, no oil leakage was observed, with the oil well retained in the structure. Previous studies have indicated that when there are oppositely charged groups in the aqueous solution, non-covalent proteoglycan complexes are formed under the effect of electrostatic attraction, (Dickinson, 2008). This protein-polysaccharide complex has greater physical stability than only protein-coating lipid droplets (Aoki et al., 2005; McClements, 2010). However, at 1.5 wt% and 2.0 wt% anionic polysaccharide additions, the samples appeared as light yellow solids with an oil-free and rough surface, and the oil droplets were embedded in a continuous network, which might be ascribed to the successful adsorption of anionic polysaccharides on the interface of BSOB to form a cross-linked network (Zhu et al., 2024).

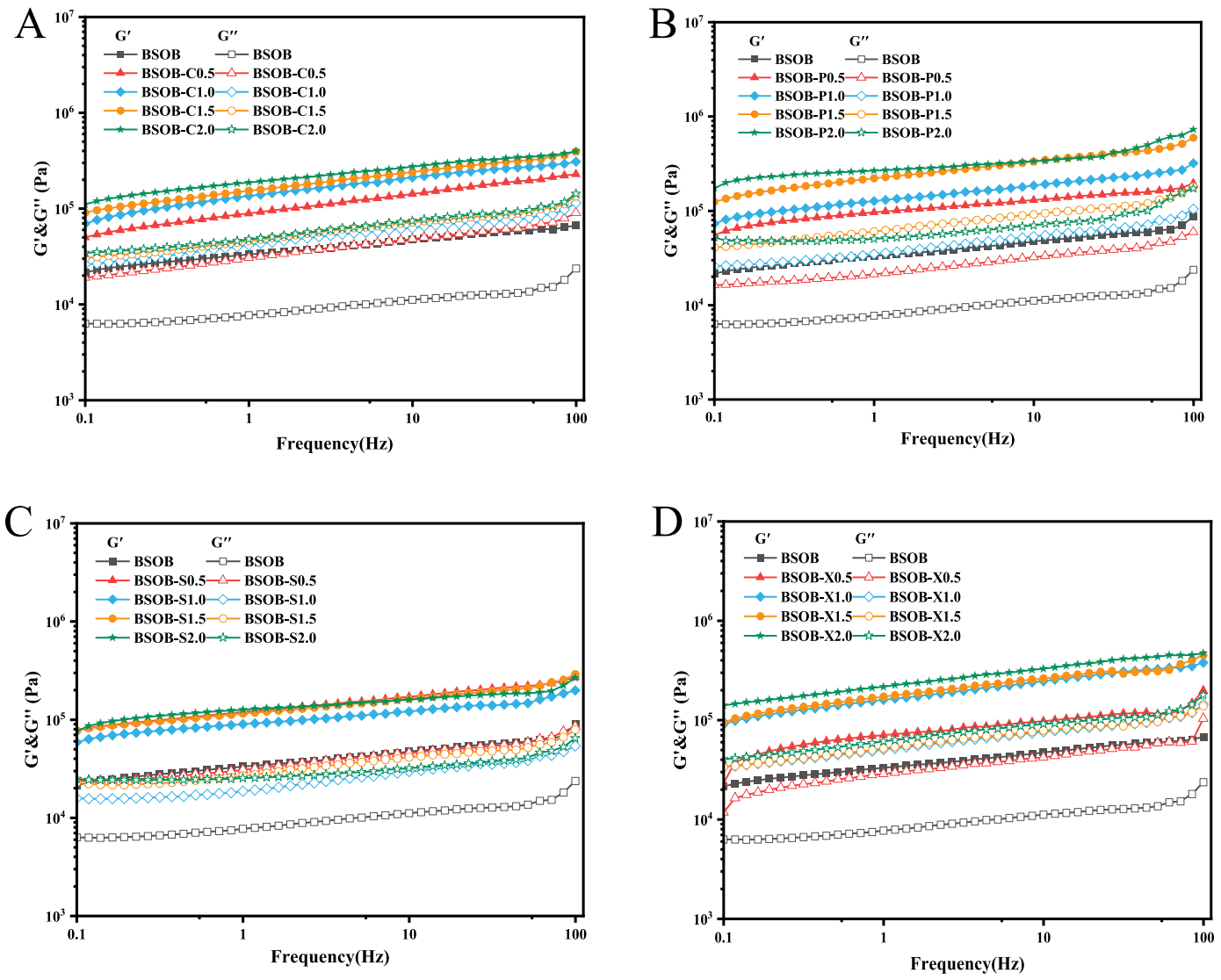

Fig. 5. Changes in the elastic modulus (G') and viscos modulus (G") of oleogels as function of frequency.

3.3. *Rheological properties during shearing in oleogels production*

Fig. 4A–D shows the apparent viscosity at various shear rates (1–100s^{-1}) during oleogels production. When varying concentrations (0.5–2.0 wt%) of anionic polysaccharides were added, the apparent viscosity of BSOB-polysaccharide emulsion decreased with increasing shear rates, exhibiting shear-thinning behavior. This might be because the emulsion network structure was disrupted, and the viscosity gradually decreased with increasing shear rate. This trend indicated that the sample exhibited characteristics of a plastic fluid (He et al., 2023). Additionally, the initial apparent viscosity value of the BSOB-polysaccharide emulsion increased with increasing anionic polysaccharide concentration. This increase could be due to the presence of inclusions or aggregates in proteins between polysaccharide molecules and the repulsion between molecules increasing the viscosity (Lizarraga et al., 2006), or positively charged proteins interacting with oppositely charged polysaccharides (Tolstoguzov, 2003). The oleogels prepared with xanthan gum exhibited higher apparent viscosity compared to those prepared with the other three polysaccharides, indicating that while the other three polysaccharides functioned merely as stabilizers for the oleogels, xanthan gum additionally acted as a thickening agent (Shi et al., 2023). With its rod-like molecular structure, xanthan gum features trisaccharide side chains that are highly entangled around the main chain. This enables it to serve as a long-chain polymer with high-viscosity characteristics, effectively enhancing the viscosity of the continuous phase and thereby altering the rheological properties of the oleogels (Cheng et al., 2024; Wen et al., 2025)

Fig. 5A–D showed the relationship between the storage modulus G′ and loss modulus G″ of the oleogels and the frequency. In the linear viscoelastic region, G′ of all samples was greater than G″, suggesting that the oleogels samples were soft solids with viscoelastic properties (Chen et al., 2023). With the gradually increasing concentration of anionic polysaccharides, G′ and G″ of the oleogel samples only increased slightly, implying that G′ of the oleogels was no longer frequency-dependent and was more elastic in property (Wang et al., 2023). At high frequency, both of G′ and G″ of the oleogels increased, exhibiting strong frequency dependence (Farooq et al., 2022). The loss factor value (Tanδ = G″/G′) of the oleogels was low, suggesting that the oleogels had a strong gel network and good stability (Liu et al., 2023).

Thixotropy describes the ability of the oleogels network to flow due to reduced viscosity under high shear force and to recover viscosity after the high shear force is removed. Thixotropy is an important rheological property for evaluating the potential application of oleogels in food manufacturing (Li et al., 2023a). To evaluate the time-dependent rheological properties and structural recovery of BSOB-based oleogels, the samples underwent altering low (0.1s^{-1}) to high (10s^{-1}) to low

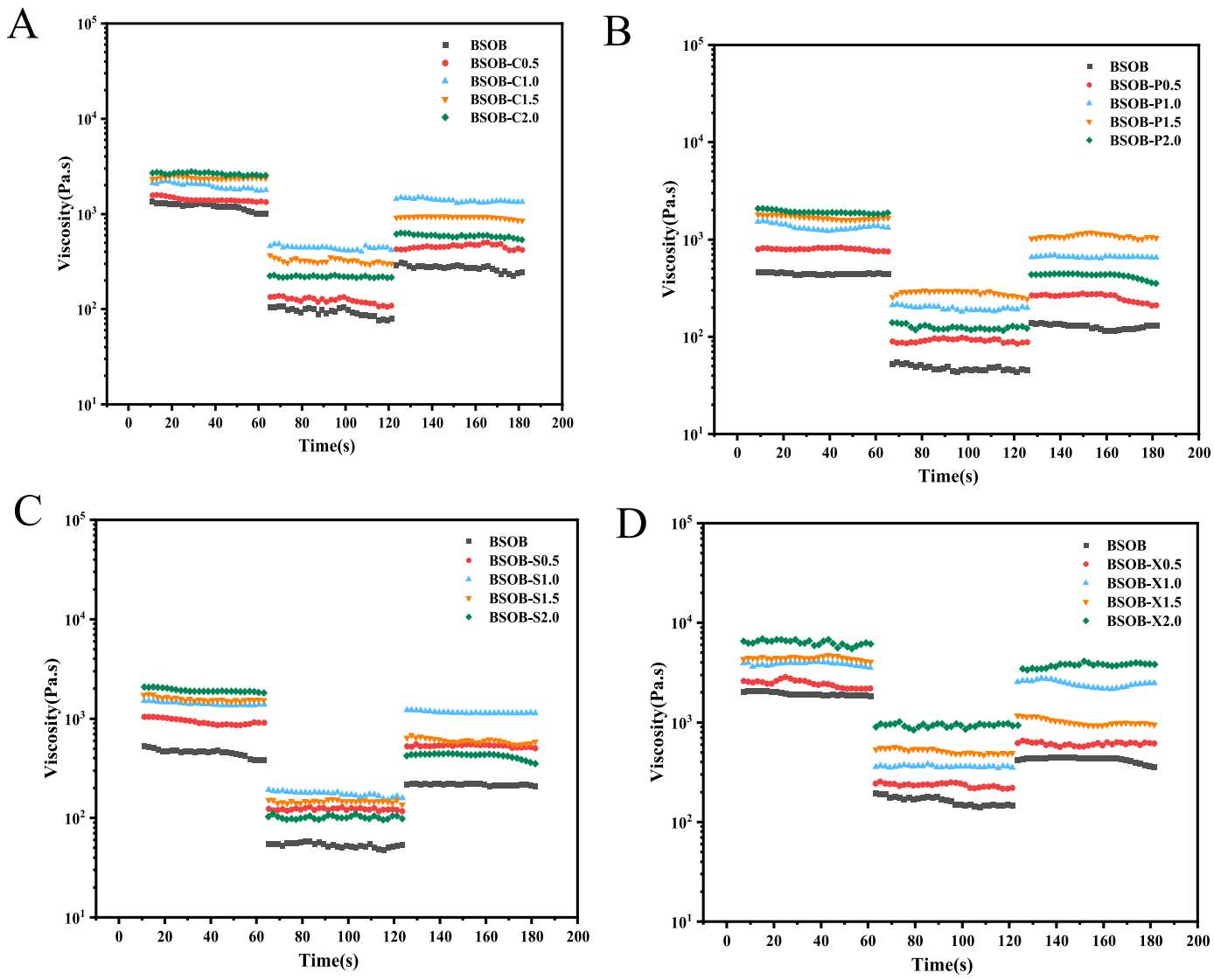

Fig. 6. In-shear structural recovery plots of the oleogels.

($0.1s^{-1}$) shear, and the changes in the apparent viscosity of the oleogels were monitored. As shown in Fig. 6, at the low shear rate in the first stage, the apparent viscosity of the oleogels slowly decreased with increasing shear time. When the shear rate was rapidly increased from the low shear rate in the first stage to the high shear rate in the second stage, the viscosity of all oleogels decreased immediately, exhibiting shear-thinning behavior, consistent with the shear scanning test values presented in Fig. 4. These results suggest that sufficiently large stress would disrupt the connection within the oleogels network structure, thus reducing its flow resistance and exhibiting shear-thinning behavior (Meng et al., 2018b). When the high shear rate in the second stage was reduced to the low shear rate in the third stage, the apparent viscosity of the oleogels partially restored, in line with reports by Farooq et al. (Farooq et al., 2022). The oleogels added with anionic polysaccharides had higher recovery rates than the control group. Specially, oleogels with BSOB-C1.0, BSOB-P1.5, BSOB-S1.0, and BSOB-X1.0 showed higher recovery rates, with satisfactory thixotropic recovery results, thus exhibiting promising application prospect in fields requiring reversible structural destruction and recovery (Liu et al., 2022).

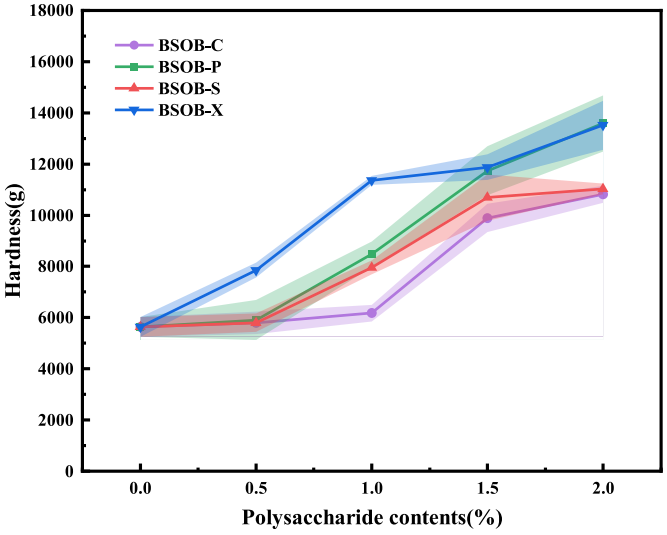

Fig. 7. Texture properties of freeze-dried samples.

3.4. Texture characteristics analysis

Hardness reflects the gel strength of the samples and the density of

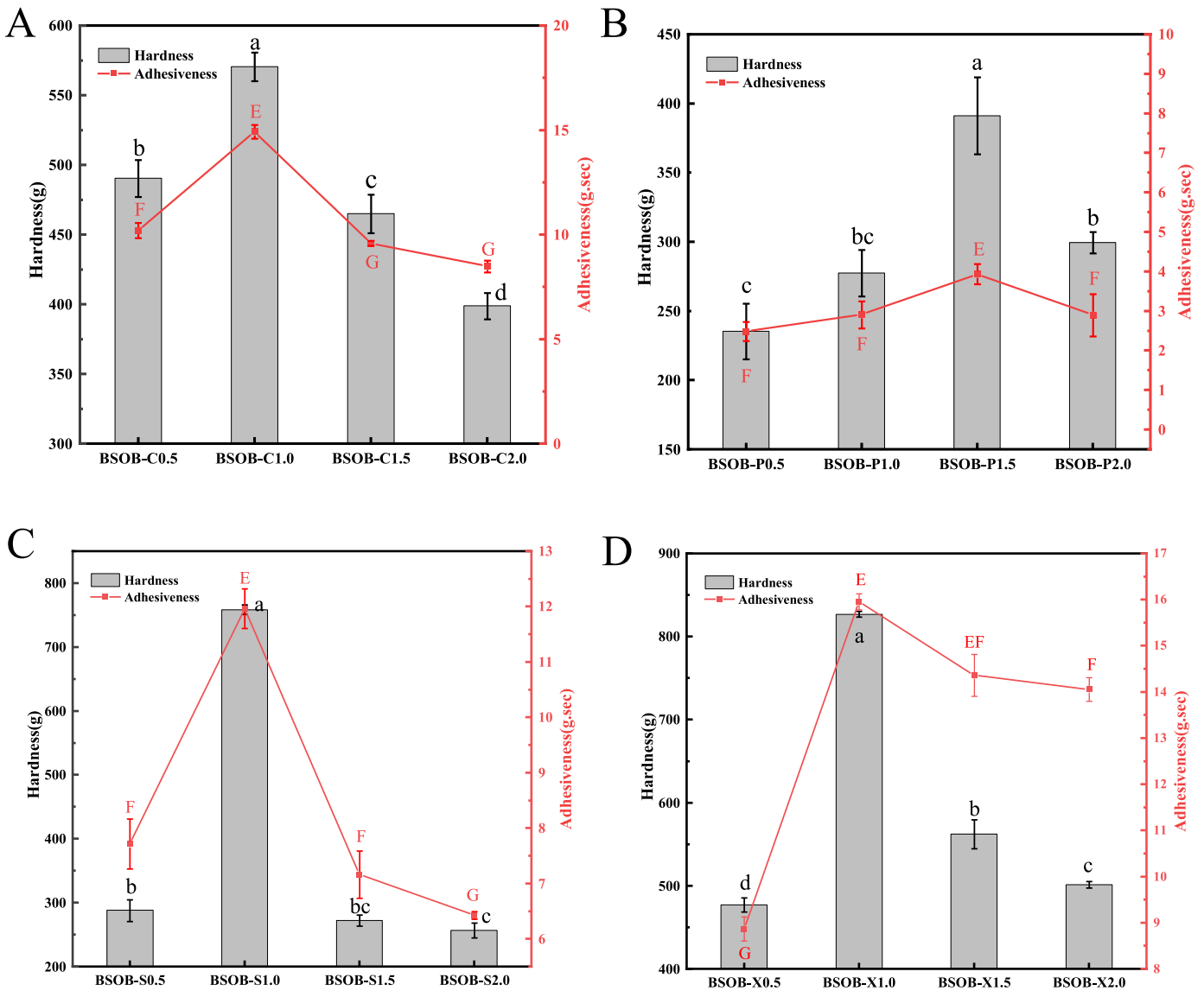

Fig. 8. Texture properties of oleogels, where the histogram (left) refers to hardness, and the line graph (right) refers to adhesiveness. Different letters (a–d) indicate significant differences ($p < 0.05$) in hardness while letters (E–G) indicate significant differences ($p < 0.05$) in Adhesiveness.

the gel network structure to a certain extent (Meng et al., 2018a). The textural properties of the freeze-dried sample mixture and the finally oleogels are shown in Figs. 7 and 8. Fig. 7 presents the hardness test results of freeze-dried samples prepared with various anionic polysaccharides. With increasing concentrations of different types of anionic polysaccharides, the hardness of the freeze-dried samples gradually increased. This increase might be attributed to the anionic polysaccharides adsorbing onto the surface of oil body proteins and forming a multilayer structure. This structure not only protected the oil body from aggregation but also reduced the damage to ice crystals at the interface during freeze-drying, further maintaining the integrity of the oil body membrane and eventually promoting the formation of a dense network structure, thereby improving the strength of the gel system (Luo et al., 2019).

The oleogels obtained by shearing the freeze-dried samples was a soft gel with low hardness and good adhesion as seen in Fig. 8. With increasing concentrations of anionic polysaccharides, the hardness of the oleogels first increased and then decreased. This pattern might occur because at low concentrations, there is insufficient polysaccharide to fully bind with the oil body protein and form a dense composite interface, resulting in the rupture of the oil body membrane. Conversely, a high concentration of anionic polysaccharides restricted the flow of oil, leading to a decrease in viscosity (Liu et al., 2022). Compared to the corresponding freeze-dried samples, the hardness of the oleogels was lower, which could be explained by the fact that the freeze-dried product has a porous network, and the oil absorption after shearing reduces the support of the network structure, thereby reducing the hardness of the corresponding oleogels (Manzocco et al., 2017; Zhao et al., 2024).

3.5. Analysis of oil holding capacity of oleogels

Another important property of oleogels is their ability to retain a high-concentration liquid oil phase. Therefore, a centrifugal stability test can be used to evaluate the impact of anionic polysaccharide addition on the stability of oleogels and to investigate the strength of the gel network structure. Oil migration within an oleogel can lead to significant quality issues and deterioration of its functional properties (Mert and Vilgis, 2021). As shown in Fig. 9, after high-speed centrifugation, only the control group (BSOB) exhibited significant oil leakage. In contrast, no obvious oil leakage was observed in the samples with added anionic polysaccharides, indicating that the inclusion of anionic polysaccharides strengthened the gel network structure, enabling the

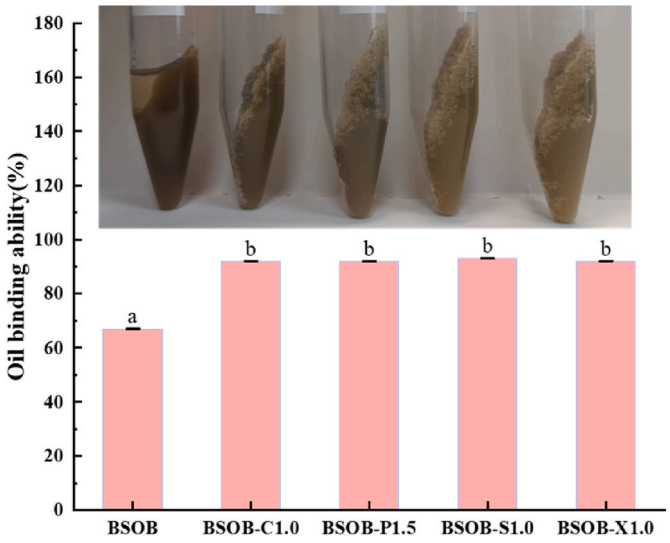

Fig. 9. Oil holding capacity of oleogels. Different letters indicate a significant difference among different samples ($P < 0.05$).

oleogels to resist deformation during centrifugation. These results suggest that the anionic polysaccharides addition significantly improved the oil-holding capacity of the oleogels (Luo et al., 2019). This improvement might be attributed to the fact that anionic polysaccharides envelop the outer layer of oil bodies, forming a dense and stable three-dimensional network structure (Zhang et al., 2023).

3.6. Analysis of oleogels microstructure

As shown in Fig. 10, the microstructure of the uncoated BSOB oleogels exhibited significant damage to oil droplets, indicating that the single-layer membrane structure of BSOB could not withstand high shear forces after freeze-drying (Farooq et al., 2023a). This result is also consistent with the observation in Fig. 6, where the viscosity of all oleogels decreased immediately as the shear rate rapidly changed from the low level in the first stage to the high level in the second stage. A large number of irregularly shaped oil droplets were observed in the BSOB oleogels (highlighted in red in Fig. 10), showing the fragile structure of BSOB, which was easy to destroy. In contrast, confocal laser scanning microscope (CLSM) observations after adding anionic polysaccharides to BSOB oleogels showed a stable network structure formed by anionic polysaccharides (highlighted in green part in Fig. 10) that enveloped most of the oil bodies, aiding in oil retention (Ding et al., 2019). Compared with the characterization results of uncoated BSOB oleogels, the addition of anionic polysaccharides effectively trapped the oil droplets within a continuous 3-D network structure, likely due to the cross-linking effect between polysaccharide molecules that secured the

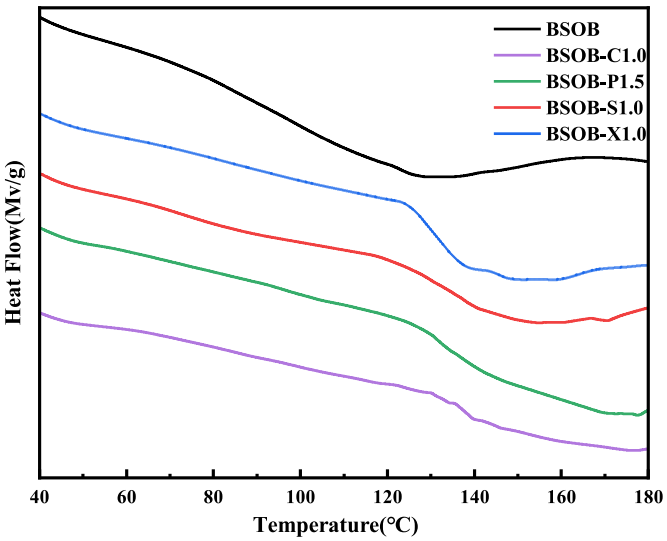

Fig. 11. DSC curves of oleogels.

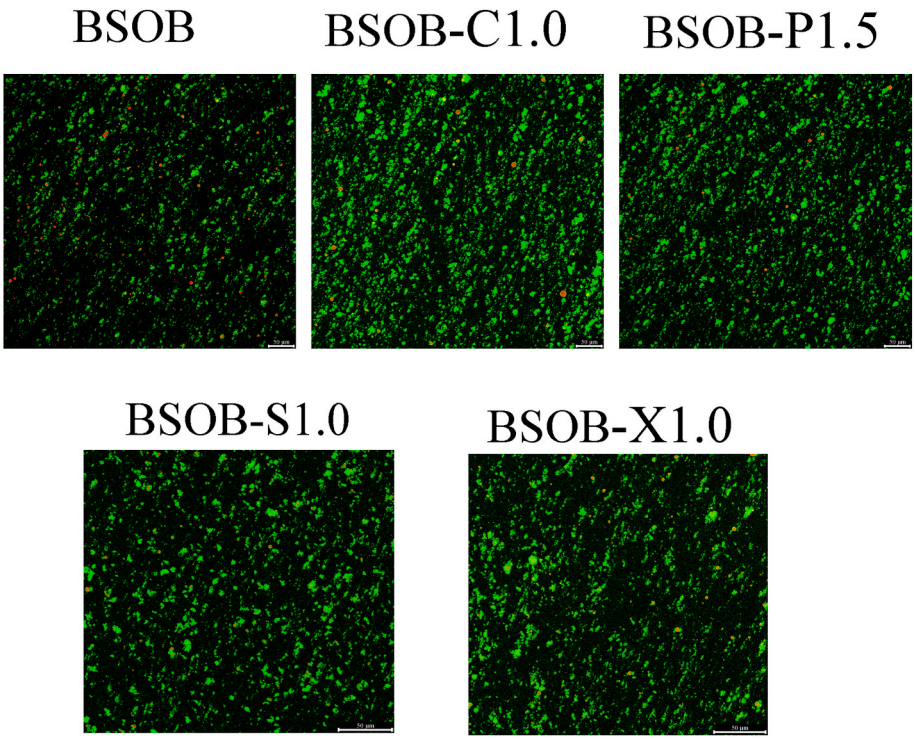

Fig. 10. CLSM micrograph of oleogels.

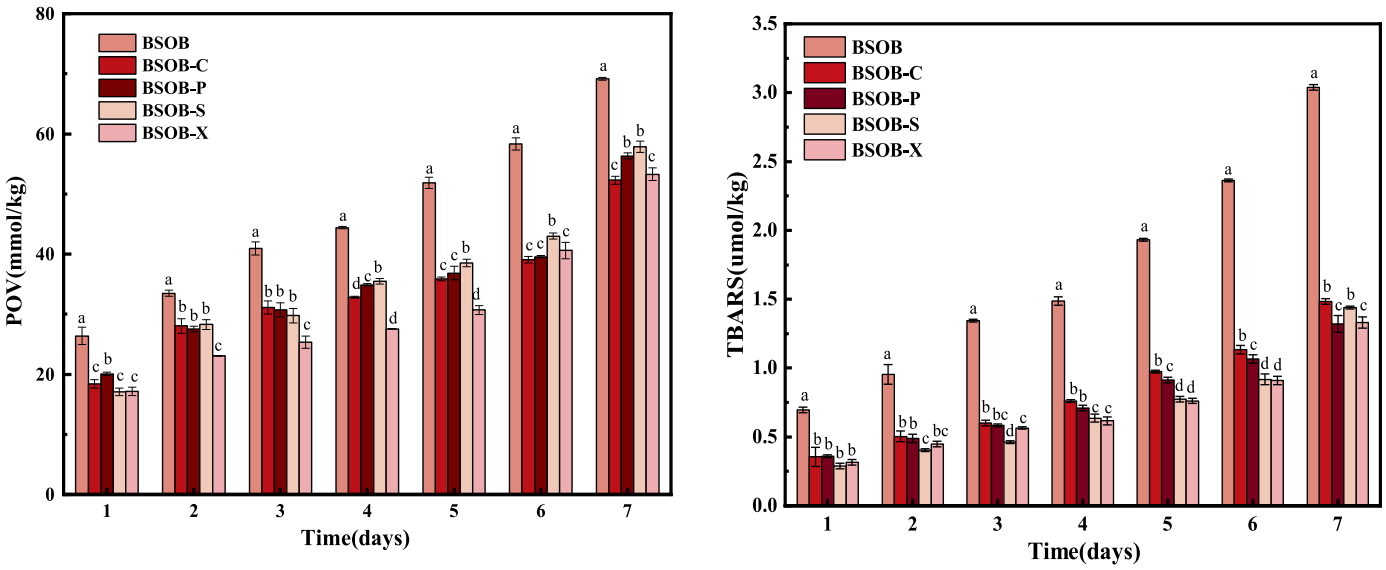

Fig. 12. Oxidative stability analysis of oleogels.

oil droplets together. Similarly, Farooq et al. used CLSM to examine the microstructure of oleogels and found significantly changes after the κ-carrageenan coating was applied (Farooq et al., 2023b). This was likely because the addition of κ-carrageenan preserved the complete single-layer membrane structure of the oil body by forming a stable interface layer, which benefited to oil retention.

3.7. Thermal stability analysis of oleogels

Fig. 11 displays the DSC curve of the oleogels. The thermal denaturation temperature value (Td) of BSOB was 129.8 °C, indicating that BSOB underwent thermal degradation at this temperature, possibly due to the denaturation of BSOB proteins (Farooq et al., 2022). This result contrasts with a previous report that suggested the Td value of wheat germ oil body is between 100 and 105 °C (Güneş & Gülseren, 2021). This discrepancy may be attributed to differences in oil bodies and preparation methods. Notably, the Td values of BSOB-C, BSOB-P, BSOB-S and BSOB-X oleogels were significantly higher than that of uncoated BSOB, suggesting that electrostatic interactions and hydrogen bonds formed on the anionic polysaccharide-coated BSOB increase the thermodynamic stability of BSOB proteins, thereby enhancing the thermal properties of the oleogels. Moreover, the Td value of BSOB-C oleogels was the highest, which may be that the rigid ring structure of carrageenan restricts the thermal movement of the molecular chain, reduces the conformation disorder caused by heat induction, and can strengthen the double helix cohesion through hydrophobic interaction and hydrogen bonding, making the double helix not easy to spin at high temperatures, promoting oleogels network to be dense and rigid (Manzocco et al., 2017; Li et al., 2025). Some researchers have found that dense biopolymer coating and vanillin-induced cross-linking can convert plant-derived OBs into an oleogel with higher transformation peak and enthalpy values. Additionally, edible and structured oleogels based on plant-derived OBs prepared with higher concentrations of chitosan or vanillin exhibit better thermal stability (Farooq et al., 2023a).

3.8. Analysis of oxidative stability of oleogels

Peroxide is the primary reaction product of oil oxidation and rancidity. The peroxide value (POV) is commonly used to reflect the early stage of oil oxidation, while the thiobarbituric acid reaction substance (TBARS) value characterizes the secondary stage of oil oxidation. Oil oxidation and rancidity represent complex processes. Typically, both TBARS and POV value are combined to analyze the oil's oxidation process (Shuai et al., 2023). Fig. 12 exhibited the oxidative stability change of oleogel samples stored at 60 °C for 7 days, with uncoated BSOB used as the control. As seen in Fig. 12, the primary and secondary oxidation products of different oleogels generally displayed an increasing trend over time. On the 7th day of storage, the content of primary oxidation products of BSOB reached 69.183 mmol/kg, and that of secondary oxidation products was 3.039 μmol/kg. Oleogels prepared under different conditions were able to inhibit the oxidation of oil and reduce the formation of oxidation products. The highest content of primary and secondary oxidation products was 57.86 mmol/kg and 1.485 μmol/kg, respectively, while the lowest was 52.29 mmol/kg and 1.32 μmol/kg (Fig. 12A and B). Polysaccharide molecules facilitate the formation of a continuous and dense three-dimensional network structure in oleogels, which immobilizes liquid oil within the interstices of the network. This structure reduces the direct contact between oil droplets and external oxygen, thereby significantly decreasing the oxygen diffusion rate. These findings indicate that the dense oleogels network provides a protective barrier to the liquid oil, slowing down the kinetic rate at which oil molecules are converted into secondary oxidation products such as aldehydes or ketones (Li et al., 2023b). Similarly, other studies have indicated that oleogels can inhibit lipid oxidation. For instance, Farooq et al. have reported that oleogels based on plant-derived OBs prepared by adjusting the concentrations of chitosan and vanillin can prevent oil leakage from the oleogels and enhance their oxidative stability (Farooq et al., 2023a). Ma et al. also reported that oleogels prepared with soy protein isolate and varying concentrations of highland barley β-glucan can improve the oxidative stability of flaxseed oil (Ma et al., 2023).

4. Conclusion

In this study, we combined BSOB with four different concentrations of anionic polysaccharides (C, P, S, and X) through electrostatic deposition and prepared oleogels using the emulsion template method. The results showed that anionic polysaccharides effectively encapsulated BSOB, thus inhibiting their aggregation and preventing oil leakage from BSOB during oleogels preparation. Additionally, the viscosity of the BSOB emulsion increased with the increasing amount of anionic polysaccharides (0.5–2 wt%). In terms of appearance and microscopic structure, the addition of anionic polysaccharides protected the oil within the structure, demonstrating good oil holding capacity (>92 %).

Regarding texture and rheology, the oleogels prepared with C (1–1.5 wt %), P (1–1.5 wt%), S (1–1.5 wt%), and X (0.5–1 wt%) exhibited strong structural recovery performance. The texture results showed that the oleogels prepared with 1 wt% C, 1.5 wt% P, 1 wt% S, 1 wt% X displayed optimal texture characteristics. The results demonstrated that the addition of anionic polysaccharides significantly enhanced the antioxidant properties of oil, slowed down the oxidation rate, and improved oxidative stability. Moreover, the thermal stability of oleogels prepared with C was higher than those prepared with other polysaccharides, likely due to the electrostatic interaction between anionic polysaccharides and BSOB proteins, rendering the BSOB protein structure more stable and resistant to damage. Overall, our results reveal that BSOB-based oleogels developed in this study have great potential to be used as substitutes for saturated fat and trans fats in food processing.

CRediT authorship contribution statement

Jie Sun: Writing – original draft, Methodology, Investigation, Funding acquisition, Conceptualization. **Cuicui Fan:** Investigation. **Guoyou Yin:** Writing – review & editing, Validation, Project administration, Conceptualization. **Zhuofan Yang:** Visualization, Data curation. **Yulin Liu:** Methodology. **Jing Lu:** Writing – review & editing.

Declaration of competing interest

The author declares no competing financial interest.

Acknowledgment

This work was supported financially by the Pingdingshan Science and Technology Innovation Outstanding Talents Program (No. 2017010 (10.4)), Henan Key Scientific Research Projects (No. 25B550022).

Data availability

Data will be made available on request.

References

Abdollahi, M., Goli, S. A. H., & Soltanizadeh, N. (2020). Physicochemical properties of foam-templated oleogel based on gelatin and xanthan gum. *European Journal of Lipid Science and Technology, 122*(2). https://doi.org/10.1002/ejlt.201900196. Article 1900196.

Aberkane, L., Roudaut, G., & Saurel, R. (2014). Encapsulation and oxidative stability of PUFA-rich oil microencapsulated by spray drying using pea protein and pectin. *Food and Bioprocess Technology, 7*(5), 1505–1517. https://doi.org/10.1007/s11947-013-1202-9

Aoki, T., Decker, E. A., & McClements, D. J. (2005). Influence of environmental stresses on stability of O/W emulsions containing droplets stabilized by multilayered membranes produced by a layer-by-layer electrostatic deposition technique. *Food Hydrocolloids, 19*(2), 209–220. https://doi.org/10.1016/j.foodhyd.2004.05.006

Astrup, A., Magkos, F., Bier, D. M., Brenna, J. T., De Oliveira Otto, M. C., Hill, J. O., King, J. C., Mente, A., Ordovas, J. M., Volek, J. S., Yusuf, S., & Krauss, R. M. (2020). Saturated fats and health: A reassessment and proposal for food-based recommendations. *Journal of the American College of Cardiology, 76*(7), 844–857. https://doi.org/10.1016/j.jacc.2020.05.077

Barbosa, A. D., & Siniossoglou, S. (2017). Function of lipid droplet-organelle interactions in lipid homeostasis. *Biochimica et Biophysica Acta (BBA)-Mol. Cell Res., 1864*(9), 1459–1468. https://doi.org/10.1016/j.bbamcr.2017.04.001

Bascuas, S., Morell, P., Hernando, I., & Quiles, A. (2021). Recent trends in oil structuring using hydrocolloids. *Food Hydrocolloids, 118*, Article 106612. https://doi.org/10.1016/j.foodhyd.2021.106612

Chen, Y., & Ono, T. (2010). Simple extraction method of non-allergenic intact soybean oil bodies that are thermally stable in an aqueous medium. *Journal of Agricultural and Food Chemistry, 58*(12), 7402–7407. https://doi.org/10.1021/jf1006159

Chen, Z., Shi, Z., & Meng, Z. (2023). Development and characterization of antioxidant-fortified oleogels by encapsulating hydrophilic tea polyphenols. *Food Chemistry, 414*, Article 135664. https://doi.org/10.1016/j.foodchem.2023.135664

Cheng, Y., Wang, B., Lv, W., Zhong, Y., & Li, G. (2024). Effect of xanthan gum on physicochemical properties and 3d printability of emulsion-filled starch gels. *Food Hydrocolloids, 149*, Article 109613. https://doi.org/10.1016/j.foodhyd.2023.109613

Davidovich-Pinhas, M. (2019). Oil structuring using polysaccharides. *Current Opinion in Food Science, 27*, 29–35. https://doi.org/10.1016/j.cofs.2019.04.006

Demirkesen, I., & Mert, B. (2020). Recent developments of oleogel utilizations in bakery products. *Critical Reviews in Food Science and Nutrition, 60*(14), 2460–2479. https://doi.org/10.1080/10408398.2019.1649243

Dickinson, E. (2008). Interfacial structure and stability of food emulsions as affected by protein-polysaccharide interactions. *Soft Matter, 4*(5), 932–942. https://doi.org/10.1039/b718319d

Ding, J., Xu, Z., Qi, B., Cui, S., Wang, T., Jiang, L., Zhang, Y., & Sui, X. (2019). Fabrication and characterization of soybean oil bodies encapsulated in maltodextrin and chitosan-EGCG conjugates: An *in vitro* digestibility study. *Food Hydrocolloids, 94*, 519–527. https://doi.org/10.1016/j.foodhyd.2019.04.001

Farooq, S., Ijaz Ahmad, M., Zhang, Y., Chen, M., & Zhang, H. (2022). Fabrication, characterization and *in vitro* digestion of camellia oil body emulsion gels cross-linked by polyphenols. *Food Chemistry, 394*, Article 133469. https://doi.org/10.1016/j.foodchem.2022.133469

Ferreira, C. D., Ziegler, V., Lindemann, I. D. S., Hoffmann, J. F., Vanier, N. L., & Oliveira, M. D. (2018). Quality of black beans as a function of long-term storage and moldy development: Chemical and functional properties of flour and isolated protein. *Food Chemistry, 246*, 473–480. https://doi.org/10.1016/j.foodchem.2017.11.118

Güneş, R., & Gülseren, İ. (2021). FT-IR spectroscopy based investigation of stability in wheat germ oil body emulsions as affected by general processing treatments. *Journal of Food Measurement and Characterization, 15*(4), 3026–3035. https://doi.org/10.1007/s11694-021-00897-8

He, Q., Yang, Y., Wu, Y., Bai, F., Peng, C., Hou, R., Sun, Y., & Cai, H. (2023). Preparation and analysis of selenium-enriched oleogels: Preliminary evaluation of antioxidant activity and inhibition of fatty acids release. *LWT-Food Science & Technology, 186*, Article 115203. https://doi.org/10.1016/j.lwt.2023.115203

Huang, A. H. C. (2018). Plant lipid droplets and their associated proteins: Potential for rapid advances. *Plant Physiology, 176*(3), 1894–1918. https://doi.org/10.1104/pp.17.01677

Li, B., Zhou, M., Qin, H., Wu, A., Li, J., Wang, Y., & Hu, Z. (2025). Impact of Gelatin/K-carrageenan ratio in the properties of bigels for food applications. *Food and Bioproducts Processing, 153*, 315–321. https://doi.org/10.1016/j.fbp.2025.07.011

Lima, F. S. D., Kurozawa, L. E., & Ida, E. I. (2014). The effects of soybean soaking on grain properties and isoflavones loss. *LWT-Food Science & Technology, 59*(2), 1274–1282. https://doi.org/10.1016/j.lwt.2014.04.032

Liu, J., Hu, L., Xiao, Y., Liu, Y., Li, S., Zheng, M., Yu, Z., Liu, K., & Zhou, Y. (2022). Gel properties and formation mechanism of camellia oil body-based oleogel improved by camellia saponin. *Gels, 8*(8), 499. https://doi.org/10.3390/gels8080499

Liu, Z., Liu, C., Sun, X., Zhang, S., Yuan, Y., Wang, D., & Xu, Y. (2020). Fabrication and characterization of cold-gelation whey protein-chitosan complex hydrogels for the controlled release of curcumin. *Food Hydrocolloids, 103*, Article 105619. https://doi.org/10.1016/j.foodhyd.2019.105619

Liu, B., Sun, L., Jin, F., Wan, Y., Han, X., Fu, T., Guan, Y., Xie, Z., Cheng, L., Tian, B., & Feng, Z. (2023). A novel oleogel based on porous microgel from egg white. *Food Hydrocolloids, 144*, Article 109049. https://doi.org/10.1016/j.foodhyd.2023.109049

Lizarraga, M. S., Piante Vicin, D. D., González, R., Rubiolo, A., & Santiago, L. G. (2006). Rheological behaviour of whey protein concentrate and λ-carrageenan aqueous mixtures. *Food Hydrocolloids, 20*(5), 740–748. https://doi.org/10.1016/j.foodhyd.2005.07.007

Luo, S. Z., Hu, X. F., Jia, Y. J., Pan, L. H., Zheng, Z., Zhao, Y. Y., Mu, D. D., Zhong, X. Y., & Jiang, S. T. (2019). Camellia oil-based oleogels structuring with tea polyphenol-palmitate particles and citrus pectin by emulsion-templated method: Preparation, characterization and potential application. *Food Hydrocolloids, 95*, 76–87. https://doi.org/10.1016/j.foodhyd.2019.04.016

Ma, Y., Ye, F., Chen, J., Ming, J., Zhou, C., Zhao, G., & Lei, L. (2023). The microstructure and gel properties of linseed oil and soy protein isolate based-oleogel constructed with highland barley β-glucan and its application in luncheon meat. *Food Hydrocolloids, 140*, Article 108666. https://doi.org/10.1016/j.foodhyd.2023.108666

Manzocco, L., Valoppi, F., Calligaris, S., Andreatta, F., Spilimbergo, S., & Nicoli, M. C. (2017). Exploitation of κ-carrageenan aerogels as template for edible oleogel preparation. *Food Hydrocolloids, 71*, 68–75. https://doi.org/10.1016/j.foodhyd.2017.04.021

Martins, A. J., Vicente, A. A., Cunha, R. L., & Cerqueira, M. A. (2018). Edible oleogels: An opportunity for fat replacement in foods. *Food & Function, 9*(2), 758–773. https://doi.org/10.1039/C7FO01641G

McClements, D. J. (2010). Design of nano-laminated coatings to control bioavailability of lipophilic food components. *Journal of Food Science, 75*(1), 30–42. https://doi.org/10.1111/j.1750-3841.2009.01452.x

Meng, Z., Qi, K., Guo, Y., Wang, Y., & Liu, Y. (2018a). Macro-micro structure characterization and molecular properties of emulsion-templated polysaccharide oleogels. *Food Hydrocolloids, 77*, 17–29. https://doi.org/10.1016/j.foodhyd.2017.09.006

Meng, Z., Qi, K., Guo, Y., Wang, Y., & Liu, Y. (2018b). Physical properties, microstructure, intermolecular forces, and oxidation stability of soybean oil oleogels structured by different cellulose ethers. *European Journal of Lipid Science and Technology, 120*(6), Article 1700287. https://doi.org/10.1002/ejlt.201700287

Mert, B., & Vilgis, T. A. (2021). Hydrocolloid coated oleosomes for development of oleogels. *Food Hydrocolloids, 119*, Article 106832. https://doi.org/10.1016/j.foodhyd.2021.106832

Mozaffarian, D., Katan, M. B., Ascherio, A., Stampfer, M. J., & Willett, W. C. (2006). Trans fatty acids and cardiovascular disease. *New England Journal of Medicine, 354*(15), 1601–1613. https://doi.org/10.1056/NEJMra054035

Patel, A. R., Nicholson, R. A., & Marangoni, A. G. (2020). Applications of fat mimetics for the replacement of saturated and hydrogenated fat in food products. *Current Opinion in Food Science, 33*, 61–68. https://doi.org/10.1016/j.cofs.2019.12.008

Restrepo, B. J., & Rieger, M. (2015). Denmark's policy on artificial trans fat and cardiovascular disease. *American Journal of Preventive Medicine, 50*(1), 69–76. https://doi.org/10.1016/j.amepre.2015.06.018

Romero-Guzmán, M. J., Köllmann, N., Zhang, L., Boom, R. M., & Nikiforidis, C. V. (2020). Controlled oleosome extraction to produce a plant-based mayonnaise-like emulsion using solely rapeseed seeds. *LWT-Food Science & Technology, 123*, Article 109120. https://doi.org/10.1016/j.lwt.2020.109120

Shi, F., Chang, Y., Shen, J., Chen, G., & Xue, C. (2023). A comparative investigation of anionic polysaccharides (sulfated fucan, ι-carrageenan, κ-carrageenan, and alginate) on the fabrication, stability, rheology, and digestion of multilayer emulsion. *Food Hydrocolloids, 134*, Article 108081. https://doi.org/10.1016/j.foodhyd.2022.108081

Shimada, T. L., & Hara-Nishimura, I. (2015). Leaf oil bodies are subcellular factories producing antifungal oxylipins. *Current Opinion in Plant Biology, 25*, 145–150. https://doi.org/10.1016/j.pbi.2015.05.019

Shuai, X., McClements, D. J., Geng, Q., Dai, T., Ruan, R., Du, L., Liu, Y., & Chen, J. (2023). Macadamia oil-based oleogels as cocoa butter alternatives: Physical properties, oxidative stability, lipolysis, and application. *Food Research International, 172*, Article 113098. https://doi.org/10.1016/j.foodres.2023.113098

Singh, A., Auzanneau, F. I., & Rogers, M. A. (2017). Advances in edible oleogel technologies-a decade in review. *Food Research International, 97*, 307–317. https://doi.org/10.1016/j.foodres.2017.04.022

Su, C., Feng, Y., Ye, J., Zhang, Y., Gao, Z., Zhao, M., Yang, N., Nishinari, K., & Fang, Y. (2018). Effect of sodium alginate on the stability of natural soybean oil body emulsions. *RSC Advances, 8*(9), 4731–4741. https://doi.org/10.1039/C7RA09375F

Tolstoguzov, V. (2003). Some thermodynamic considerations in food formulation. *Food Hydrocolloids, 17*(1), 1–23. https://doi.org/10.1016/S0268-005X(01)00111-4

Wältermann, M., & Steinbüchel, A. (2005). Neutral lipid bodies in prokaryotes: Recent insights into structure, formation, and relationship to eukaryotic lipid depots. *Journal of Bacteriology, 187*(11), 3607–3619. https://doi.org/10.1128/JB.187.11.3607-3619.2005

Wang, T., Wang, N., Dai, Y., Yu, D., & Cheng, J. (2023). Interfacial adsorption properties, rheological properties and oxidation kinetics of oleogel-in-water emulsion stabilized by hemp seed protein. *Food Hydrocolloids, 137*, Article 108402. https://doi.org/10.1016/j.foodhyd.2022.108402

Wen, X., Zhang, F., Xu, W., Chen, W., Ren, S., Hou, Z., Wang, C., He, J., Wang, Y., Xu, D., & Sun, B. (2025). Xanthan gum-regulated milk minerals-loaded triple-phase S/O/W emulsion with film-like structure: Microstructure, thermal and freeze-thaw stability, and calcium bioaccessibility. *Food Hydrocolloids, 173*, Article 112250. https://doi.org/10.1016/j.foodhyd.2025.112250

Wu, N., Yang, X., Teng, Z., Yin, S., Zhu, J., & Qi, J. (2011). Stabilization of soybean oil body emulsions using κ, ι, λ-carrageenan at different pH values. *Food Research International, 44*(4), 1059–1068. https://doi.org/10.1016/j.foodres.2011.03.019

Wu, L., Yue, Q., Kang, M., Zhong, M., Qi, B., & Li, Y. (2022). Stabilization of soybean and peanut oil bodies using apple pectin under acidic conditions. *Colloids and Surfaces A: Physicochemical and Engineering Aspects, 655*, Article 130263. https://doi.org/10.1016/j.colsurfa.2022.130263

Yang, N., Zhang, Y., Su, C., Zhu, C., Jia, J., & Nishinari, K. (2023). The effect of sodium alginate on the nanomechanical properties and interaction between oil body droplets studied using atomic force microscopy. *Food Hydrocolloids, 140*, Article 108587. https://doi.org/10.1016/j.foodhyd.2023.108587

Zambrano, J. C., & Vilgis, T. A. (2023). Tunable oleosome-based oleogels: Influence of polysaccharide type for polymer bridging-based structuring. *Food Hydrocolloids, 137*, Article 108399. https://doi.org/10.1016/j.foodhyd.2022.108399

Zembyla, M., Murray, B. S., & Sarkar, A. (2020). Water-in-oil emulsions stabilized by surfactants, biopolymers and/or particles: A review. *Trends in Food Science & Technology, 104*, 49–59. https://doi.org/10.1016/j.tifs.2020.07.028

Zhang, S., Xin, M., Wang, Z., Dong, X., Yang, C., Liu, H., Fan, H., Liu, T., & Wang, D. (2023). Tiger nut oil-based oil gel: Preparation, characterization, and storage stability. *Foods, 12*(22), 4087. https://doi.org/10.3390/foods12224087

Zhang, Y. M., Yang, N., Xu, Y., Wang, Q., Huang, P., Nishinari, K., & Fang, Y. P. (2019). Improving the stability of oil body emulsions from diverse plant seeds using sodium alginate. *Molecules, 24*(21), 3856. https://doi.org/10.3390/molecules24213856

Zhao, W., Wei, Z., & Xue, C. (2024). Foam-templated oleogels constructed by whey protein isolate and xanthan gum: Multiple-effect delivery vehicle for Antarctic krill oil. *International Journal of Biological Macromolecules, 256*, Article 128391. https://doi.org/10.1016/j.ijbiomac.2023.128391

Zhu, J., Li, X., Liu, L., Li, Y., Qi, B., & Jiang, L. (2022). Preparation of spray-dried soybean oil body microcapsules using maltodextrin: Effects of dextrose equivalence. *LWT-Food Science & Technology, 154*, Article 112874. https://doi.org/10.1016/j.lwt.2021.112874

Zhu, J., Liu, L., Li, X., Zhang, Q., Wang, Z., Chen, N., Wang, H., Xie, F., Qi, B., & Jiang, L. (2024). Construction of soybean oil bodies-xanthan gum composite oleogels by emulsion-templated method: Preparation, characterization, and stability analysis. *Food Hydrocolloids, 149*, Article 109526. https://doi.org/10.1016/j.foodhyd.2023.109526

Farooq, S., Ahmad, M. I., Zhang, Y., & Zhang, H. (2023b). Impact of interfacial layer number and Schiff base cross-linking on the microstructure, rheological properties and digestive lipolysis of plant-derived oil bodies-based oleogel. *Food Hydrocolloids, 138*, Article 108473. https://doi.org/10.1016/j.foodhyd.2023.108473

Farooq, S., Ahmad, M. I., Zhang, Y., Chen, M., & Zhang, H. (2023a). Preparation, characterization and digestive mechanism of plant-derived oil bodies-based oleogels structured by chitosan and vanillin. *Food Hydrocolloids, 136*, Article 108247. https://doi.org/10.1016/j.foodhyd.2022.108247

Li, X., Guo, G., Zou, Y., Luo, J., Sheng, J., Tian, Y., & Li, J. (2023b). Development and characterization of walnut oleogels structured by cellulose nanofiber. *Food Hydrocolloids, 142*, Article 108849. https://doi.org/10.1016/j.foodhyd.2023.108849

Li, J., Xi, Y., Wu, L., & Zhang, H. (2023a). Preparation, characterization and in vitro digestion of bamboo shoot protein/soybean protein isolate based-oleogels by emulsion-templated approach. *Food Hydrocolloids, 136*, Article 108310. https://doi.org/10.1016/j.foodhyd.2022.108310